Irregularities and power law distributions in the breathing pattern in preterm and term infants

U. FREY,[1] M. SILVERMAN,[1] A. L. BARABÁSI,[2] AND B. SUKI[3]
[1]*Department of Child Health, Leicester University, Leicester LE2 7LX, United Kingdom;*
[2]*Department of Physics, University of Notre Dame, South Bend, Indiana 46556; and*
[3]*Department of Biomedical Engineering, Boston University, Boston, Massachusetts 02215*

Frey, U., M. Silverman, A. L. Barabási, and B. Suki. Irregularities and power law distributions in the breathing pattern in preterm and term infants. *J. Appl. Physiol.* 86(3): 789–797, 1998.—Unlike older children, young infants are prone to develop unstable respiratory patterns, suggesting important differences in their control of breathing. We examined the irregular breathing pattern in infants by measuring the time interval between breaths ("interbreath interval"; IBI) assessed from abdominal movement during 2 h of sleep in 25 preterm infants at a postconceptional age of 40.5 ± 5.2 (SD) wk and in 14 term healthy infants at a postnatal age of 8.2 ± 4 wk. In 10 infants we performed longitudinal measurements on two occasions. We developed a threshold algorithm for the detection of a breath so that an IBI included an apneic period and potentially some periods of insufficient tidal breathing excursions (hypopneas). The probability density distribution (***P***) of IBIs follows a power law, ***P***(IBI)~IBI$^{-\alpha}$, with the exponent α providing a statistical measurement of the relative risk of insufficient breathing. With maturation, α increased from 2.62 ± 0.4 at 41.2 ± 3.6 wk to 3.22 ± 0.4 at 47.3 ± 6.4 wk postconceptional age, indicating a decrease in long hypopneas (for paired data $P = 0.002$). The statistical properties of IBI were well reproduced in a model of the respiratory oscillator on the basis of two hypotheses: *1*) tonic neural inputs to the respiratory oscillator are noisy; and *2*) the noise explores a critical region where IBI diverges with decreasing tonic inputs. Accordingly, maturation of infant respiratory control can be explained by the tonic inputs moving away from this critical region. We conclude that breathing irregularities in infants can be characterized by α, which provides a link between clinically accessible data and the neurophysiology of the respiratory oscillator.

control of breathing; apnea; hypopnea; neural network

IT IS KNOWN THAT IN NEWBORNS and premature infants unstable respiratory patterns tend to decline with age, suggesting important developmental differences in respiratory regulation during early postnatal life (3, 15). A pattern of regular breathing interrupted by periods of insufficient breathing (hypopneas) or apneas is common. The respiratory rhythm is generated in the central nervous system by a group of respiratory neurons that forms a neural oscillator and drives the respiratory muscles. It has been proposed that immaturity of these brain stem rhythm generators (11, 13) and immature central and peripheral chemoreceptors (e.g., Ref. 12) may be the major underlying factors responsible for apnea or hypopnea in infants. However, the relationship between the maturation of respiratory-related central and peripheral neural networks and breathing pattern is poorly understood. This is because measurements of breathing pattern rely on noninvasive techniques, which have limitations regarding both the detection and quantitation of breathing movements. Further difficulties originate from the analysis of the complex dynamics of breathing in infants, which is usually arbitrary rather than being based on an understanding of respiratory brain stem function.

A physiologically justifiable parameter is needed to describe the dynamics of breathing in infants for clinical purposes. Recently, Szeto et al. (25) proposed that the fetal irregular breathing pattern in lambs is similar to fractal processes. The purpose of our study was to further develop this concept and to apply statistical approaches to the analysis of the breathing pattern in newborn human infants. To determine whether the statistical parameters derived from the breathing pattern in infants are physiologically justifiable and capable of detecting maturational changes in respiratory control, we developed a model of the neuronal respiratory oscillator that is able to account for the measured data. Our analysis may provide a key to the neurophysiological origins of the irregularities and their statistical properties observed in the breathing patterns in infants.

METHODS

The study included experiments and related analysis of the data as well as modeling with involved numerical simulations. First, we examined whether the irregular breathing pattern in infants could be described by simple power law distributions in infants as proposed by Szeto et al. (25) for lambs and whether parameters of the distributions changed during age, as an expression of maturation. In comparison to term infants, we also examined whether these indexes were different in preterm infants, who are known to be at risk of apneas. In the modeling studies, we aimed to develop a neural network model that could explain the fluctuations in frequency and amplitude of the phrenic output with statistical properties similar to those observed in the breathing pattern in infants.

Experimental Study

Subjects. We analyzed 32 recordings of abdominal movements in 25 preterm infants who were undergoing polygraphic measurements for clinical indications because of their prematurity at a mean postconceptional age (PCA) of 40.5 ± 5.2 (SD) wk and a postnatal age (PNA) of 11.7 ± 6.6 wk. Eleven of these infants had been ventilated for fewer than 3 days and had no major lung problems, and 14 infants had chronic lung disease of prematurity. None of the infants had severe cerebral impairment or intracerebral hemorrhage. Nine were treated with caffeine (5 mg·kg^{-1}·day^{-1}) because of previous apneas. We also assessed 18 sets of abdominal

movements in 15 healthy full-term infants at PNA of 8.2 ± 4 wk. The studies were authorized by the ethical committees of the Hammersmith Hospital (London, UK), where the data in preterm infants were assessed, and the Leicestershire Health Authority (Leicester, UK), where the breathing pattern in the healthy term infants was examined. Parental consent was obtained for all the studies.

Measurements. During a 2-h session of sleep, abdominal movements were assessed by using a noninvasive sensor system, which is based on the Hall effect (modified Densa monitoring system, DMS 100, Densa, Clywd, UK). The DMS 100 monitoring system was tested regarding its linear properties and time constants by using a mechanical analog consisting of a sinusoidal pump connected to a flow transducer (Honeywell AWM5000 series microbridge mass airflow sensor, range 0–20 l/min, sensitivity 0.2 $V \cdot l^{-1} \cdot min^{-1}$) and a Laerdal mannikin, to which the DMS 100 transducer was attached in the same manner as during the measurements in infants. The absolute amplitude of the DMS 100 transducer output was found to be dependent on strap tension and position. However, once transducer position was fixed, the transducer behaved linearly within the operating range. Therefore, the relative volume changes resulted in proportional changes in output voltage in the operating range. This fact made it possible to compare relative (but not absolute) changes in volume excursion even when strap tension and position varied among subjects or during measurements in the same infants at different ages. Regarding the frequency response, the Hall effect transducer itself behaves as a zero-order system; i.e., it has a flat frequency response up to 5 Hz.

To account for the fact that only relative changes within the operating range and not absolute changes were detectable in a linear manner, a special algorithm was designed to detect a breath in infants. "Interbreath intervals" (IBIs) were defined as the time interval between two significant tidal excursions (Fig. 1). The window algorithm to detect a significant tidal excursion (breath) was designed as follows: *1*) abdominal movements were recorded with 15-Hz sampling frequency; *2*) mean and SD of the tidal excursions in a time window of 120 s were assessed; and *3*) the threshold to detect a peak (breath) was set as the mean + 1 SD. The time intervals that defined the IBIs were then calculated between these significant tidal excursions. The window moved along the time series in a nonoverlapping manner. This algorithm includes small (<1 SD) tidal excursions, which we defined as hypopneas between two significant breaths.

Data analysis. Data sets with movement artifacts were not included in the study. During data collection, infants underwent several sleep cycles. Periods of different sleep stages were not analyzed separately (see DISCUSSION).

IBIs were displayed as a function of breath number as follows. The IBI between *breaths 1* and *2* was assigned to *breath 1*, the IBI between *breaths 2* and *3* was assigned to *breath 2*, and so on. A 120-min sequence of abdominal movements resulted in a time series of between ~1,000 and 7,000 IBI data points. Two examples of the IBI time series (subset of 750 IBIs) measured in the same preterm infant with clinically severe breathing irregularities at PCA of 39 wk and after improvement at 61 wk, are shown in Fig. 2. Both time series demonstrate irregular breathing, with many IBI spikes corresponding to long hypopneas. To quantify these differences we compared the probability density distribution functions of the IBI time series, ***P***(IBI), in Fig. 3*A*, which were obtained by normalizing the histogram of the IBIs so that the area under the curve was one. Because of the long tail of ***P***(IBI) for large IBI, we also plotted ***P***(IBI) on a log-log scale, where the widths of the histogram bins were selected to be equidistant on a log-log scale. For large IBIs, ***P***(IBI) decreases linearly on the log-log plot (Fig. 3*B*), which means

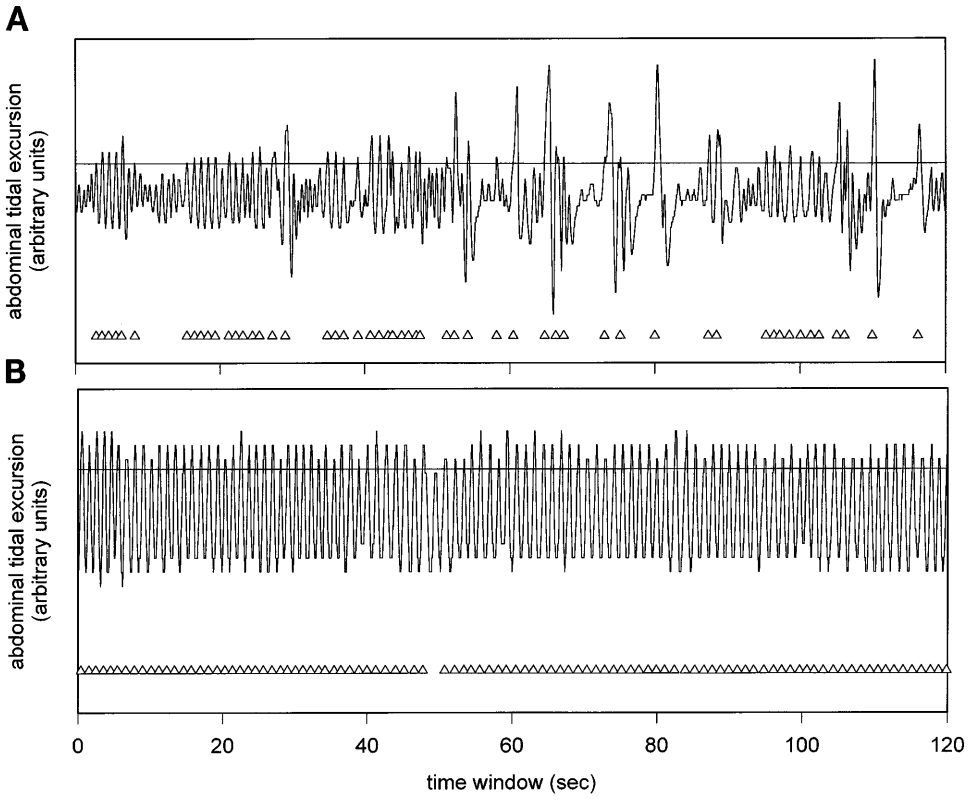

Fig. 1. Representative examples of abdominal movements in 2 healthy infants. *A*: irregular breathing (e.g., in rapid-eye-movement sleep). *B*: quiet tidal breathing. Threshold algorithm was calculated from mean + 1 SD of abdominal signal (solid line) in a nonoverlapping moving time window of 120 s. △, Detected breaths. Abdominal tidal excursions that failed to reach threshold were not counted as breaths and led to longer interbreath intervals (IBIs) between 2 significant tidal excursions.

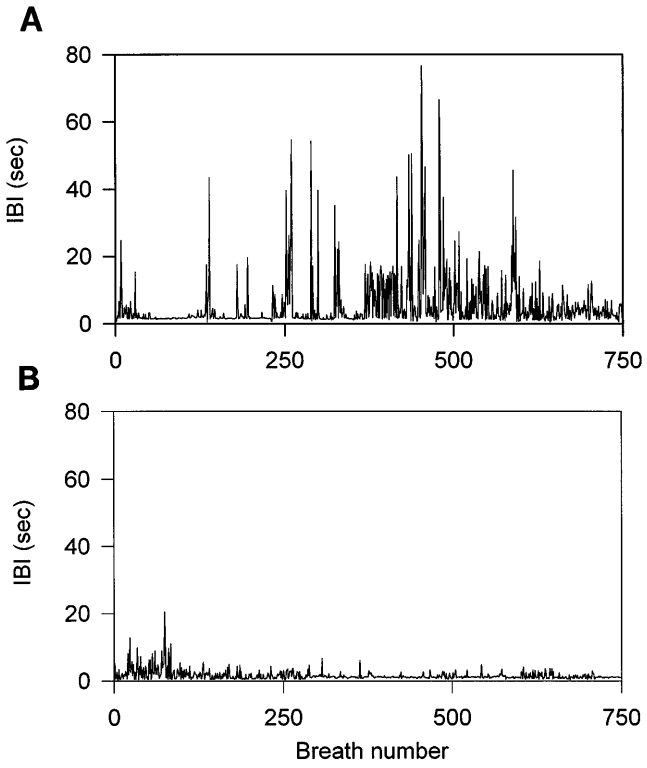

Fig. 2. Examples of IBIs (extract of 750 IBIs) as a function of breath number. IBI time series are shown in a preterm infant at 2 postconceptional ages (PCA), 39 (*A*) and 61 wk (*B*). Note that IBI represents interval between 2 significant tidal excursions (i.e., hypopnea) rather than time of an apnea (see Fig. 1).

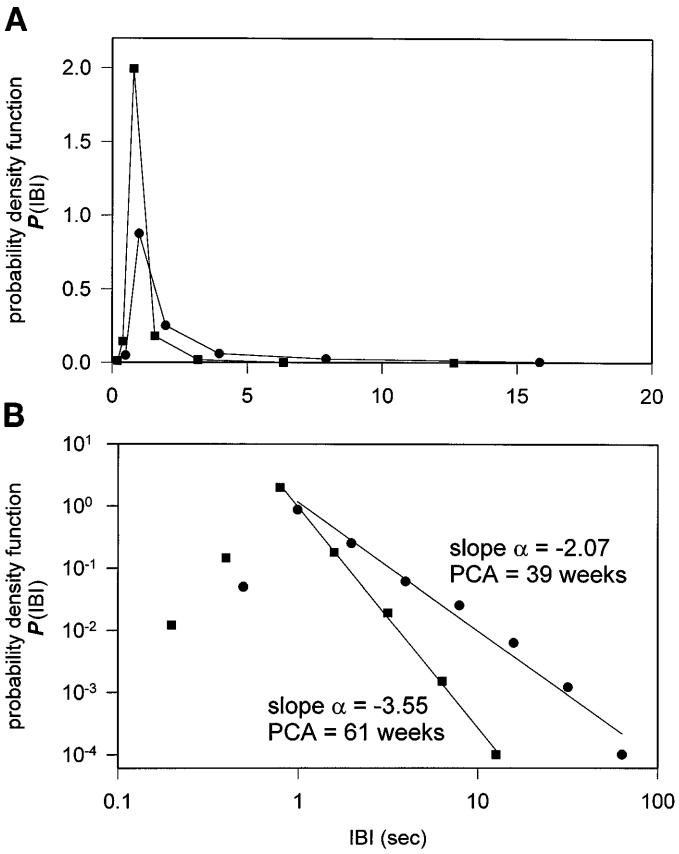

Fig. 3. Probability density distribution function [$\boldsymbol{P}$(IBI)] in linear (*A*) and in log-log presentation (*B*). Exponent α represents slope of linear regression fit through long tail of distribution [$\boldsymbol{P}$(IBI)~IBI$^{-\alpha}$]. α changed from 2.07 at 39 wk to 3.55 at 61 wk.

that the distribution has a power law tail, which can be described as follows

$$\boldsymbol{P}(\text{IBI}) \sim \text{IBI}^{-\alpha}$$

where α is the exponent in the power law and represents the slope of the linear regression through the long tail of the probability density distribution on a log-log graph. If α is small, the long tail of $\boldsymbol{P}$(IBI) decreases very slowly. Hence, the probability that an infant will have an hypopnea much longer than the mean can be orders of magnitude higher than if $\boldsymbol{P}$(IBI) followed a normal distribution (5). With increasing α, representing a steeper tail, the distribution of IBI will gradually become closer to a normal distribution.

Analysis of group data. In 10 healthy term infants, 2 sequences were recorded in the same night to determine short-term repeatability. Short-term repeatability was presented in a Bland-Altman plot and was expressed as SE of differences between the two observation periods. To determine the effect of maturation, measurements were performed longitudinally on two different occasions in seven preterm and three term infants (Table 1). Two of the preterm infants had had caffeine but on both occasions. The corresponding values of α were compared using a paired *t*-test. To test the effect of prematurity on α independent of PNA, we compared the subgroup of 10 preterm infants in which the measurements were recorded before 40 wk PCA to the group of 15 healthy infants. The two groups were significantly different in gestational age (age at birth) and in PCA and but not in PNA. The values of α in the groups were compared by using a *t*-test.

Modeling Study

We propose a mechanism to explain how the power law distribution of IBI in infants could originate from the neural respiratory network in the brain stem. To reproduce the observed irregularities, we modified the neural oscillator model proposed by Botros and Bruce (4), which transforms tonic neural inputs (TNI) into a regular rhythm and hence breathing (22). The model consists of five coupled nonlinear differential equations corresponding to the activities of five

Table 1. *Subject characteristics*

Groups	*n*	GA, wk	PCA, wk	PNA, wk	α
Term infants	15	40.1 ± 1.4[a]	48.9 ± 4.5[b]	8.8 ± 4.1[c]	2.87 ± 0.4[d]
Preterm infants	10	29.4 ± 3.8[a]	36.1 ± 2.9[b]	6.6 ± 4.3[c]	2.52 ± 0.2[d]
Longitudinal data					
1st measurement	10	31.5 ± 6.8	41.2 ± 3.6[e]	9.3 ± 5.1[f]	2.62 ± 0.4[g]
2nd measurement	10	31.5 ± 6.8	47.3 ± 6.4[e]	12.6 ± 5.6[f]	3.22 ± 0.4[g]

Values are means ± SD. *n*, no. of infants; GA, gestational age; PCA, postconceptional age; PNA, postnatal age; α, measure of relative risk of insufficient breathing. In a subgroup of preterm infants, measurements were made before term (40 wk). This group was significantly different from healthy term group in GA ([a]$P < 0.001$, *t*-test) and PCA ([b]$P < 0.001$, *t*-test) but not in PNA ([c]$P = 0.22$, *t*-test); $P = 0.29$, Mann-Whitney *U*-test. In this preterm group, α was significantly lower ([d]$P < 0.05$, *t*-test), showing a weak independent effect of prematurity on breathing pattern. In longitudinal data, PCA ([e]$P < 0.001$, *t*-test), PNA ([f]$P < 0.001$, *t*-test), and α ([g]$P < 0.002$, *t*-test) were significantly smaller at occasion of 1st measurement.

neuronal groups in the respiratory center. The ramp-inspiratory neuronal group provides periodic outputs to the phrenic nerve similar to measured data. Therefore, we solve the network in the time domain by using Matlab (Mathwork, Natick, MA) and, from the steady-state solution, take the time interval between the peaks of the output of the ramp-inspiratory neurons as proportional to IBI. However, after a short transient period, the solution of the network is a periodic waveform without any irregularities. Thus, to mimic irregularities in IBI, we add a zero-mean noise to the TNI of the first or ramp-inspiratory neuronal group (TNI_1). In this simple model (*model A*), we assumed that the noise remains constant over one cycle of the oscillator, an assumption that may be an oversimplification. Indeed, the work of Hoop et al. (16) suggests that neural noise is not constant but does vary within the respiratory cycle, most likely because of varying chemoreceptor responses. We tested this hypothesis (*model B*) by varying noise amplitude within the respiratory cycle.

In *model A*, we calculated the IBIs from the steady-state solution, whereas in *model B* we continuously solved the network without discarding the transients. The model parameters are summarized in Table 2. The parameters were the same as previously described (4), except for TNI_1 (see Table 2). In *model A*, we used a mean value of $TNI_1 = 0.12$ with a uniformly distributed noise (SD = 0.07) superimposed on TNI_1, which was constant within one respiratory cycle. In *model B*, we used a mean value of $TNI_1 = 5$ with a uniformly distributed noise (SD = 4), which changes, on average, four times within the respiratory cycle.

RESULTS

Experimental Study

A typical example of how breathing irregularity and the corresponding ***P***(IBI) change with maturation is shown in Figs. 2 and 3, respectively. It is evident even visually that the IBIs at PCA of 61 wk appear significantly less irregular, with a maximum of only ~21 s compared with ~70 s in the IBI sequence at PCA of 39 wk. Both distributions have a peak slightly above 1 s, indicating that the primary breathing rate is just below 1 Hz. The tail of the distribution changes significantly with maturation: α increases in the same infant with age (from PCA = 39 wk to PCA = 61 wk) by almost a factor of two (2.07 vs. 3.55).

Table 2. *Neural network modeling*

Source Group	Target Group I	L-I	p-I	E	e-I	TNI
I	0.7	1.361	0	−0.729	−1.8	**5.044**
L-I	−5	2.3	0	0	0	−2.2
p-I	1.719	−3	1.54	0	−2.15	3.989
E	1.371	−0.793	−1.351	1.55	0	4.140
e-I	0	−2.056	−2.254	−2.254	0.65	2.193

Model parameters according to Botros and Bruce (4) are as follows: I, inspiratory neuronal group; L-I, late inspiratory neuronal group; p-I, postinspiratory neuronal group; E, expiratory neuronal group; e-I, early inspiratory neuronal group; and TNI, tonic neural input. *Columns 1–5* show values for connection weighting factors (W*i*, *j*), where *i* is source group and *j* is target group. In original Botros and Bruce model (4), TNI in 1st or ramp-inspiratory neuronal group (TNI_1) was 5.044. In *model A*, we used a mean value of $TNI_1 = 0.12$ with a uniformly distributed noise (SD = 0.07) superimposed on TNI_1 that was constant within 1 respiratory cycle. In *model B*, we used a mean value of $TNI_1 = 5$ with a uniformly distributed noise (SD = 4) that changes, on average, 4 times within respiratory cycle.

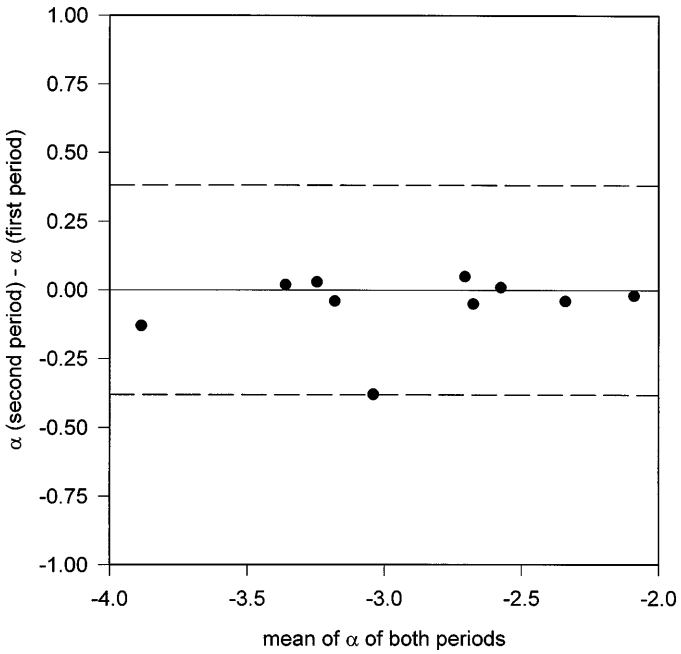

Fig. 4. Short-term repeatability in 10 healthy term infants. Differences in α of power law probability density distribution assessed during 2 periods of 2 h in same infant are presented as a function of mean of α of both periods (Bland-Altman plot). Dashed lines, 95% confidence intervals. SE of differences = 0.04.

In both the healthy and preterm infants, the power law model provided an excellent description of the long tails of the IBI distributions. In all subjects the mean (±SD) correlation coefficient (r^2) through the long tail of ***P***(IBI) was 0.973 ± 0.025. On average, the linear regression was fitted through 6.4 ± 1.4 data points (bins).

The short-term repeatability of α within a single night was remarkably high in 10 healthy infants, as shown in a Bland-Altman plot in Fig. 4 and expressed by the SE of the differences of 0.04.

The values of α ranged from 2.07 to 3.80, with a mean ± SD of 2.74 ± 0.47, and increased with PCA (Fig. 5) but showed a large variability in both the preterm and the term healthy infants. In longitudinal data sets in 10 infants, α increased statistically significantly ($P = 0.002$) (Table 1). PNA was the most important determinant factor for α (Fig. 5). In the group of measurements performed in preterm infants before a PCA of 40 wk, α was significantly smaller ($P < 0.05$) than in the group of term healthy infants of similar PNA, demonstrating a weak independent effect of prematurity on α (Table 1).

Modeling Study

The IBI time series simulated by using *model A* are shown in Fig. 6*A*. Similar to the findings in infants (cf. Fig. 2*A*), *model A* reproduces the occurrences of high spikes. ***P***(IBI) also followed a power law with α = 2.28 (Fig. 6*B*). However, *model A* may not be physiological because TNI may fluctuate within the respiratory

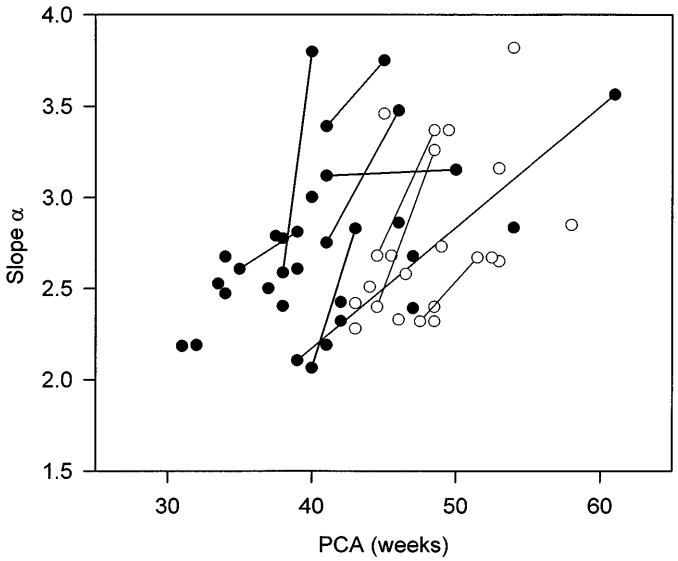

Fig. 5. Exponent α as function of PCA in preterm infants (●) and healthy term infants (○). Longitudinal data points from same subjects are connected with lines (10 subjects). Change in α in 10 longitudinal data sets during maturation was significant ($P = 0.002$, paired *t*-test).

cycle. By using *model B*, in which noise changed within the respiratory cycle, we obtained large variations in phrenic amplitude (Fig. 7*A*) similar to those observed in the measured data (see Fig. 1). By using our threshold algorithm, ***P***(IBI) showed a power law distribution with $\alpha = 3.46$ (Fig. 7*B*).

DISCUSSION

Newborns and premature infants are prone to develop unstable breathing patterns that disappear with age, suggesting that there are important developmental processes in the regulation of breathing during postnatal life (3, 11). The assessment of breathing in infants is limited by the need to use noninvasive techniques. Further difficulties originate from the analysis of the complex dynamics of breathing in infants. Analysis techniques are often arbitrary rather than being based on an understanding of respiratory brain stem function. Ideally, flow at the airway opening should be measured to determine the amplitude of breathing. The process of applying a measurement device to the face is disturbing so that often abdominal movements alone are measured to determine the breathing pattern in infants. Under these conditions the definition of hypopnea presents difficulties. Arbitrary threshold techniques for detecting abdominal signals are prone to error because calibrating and quantifying absolute abdominal movements are imprecise. It is easier to assess relative changes in abdominal movements to calculate IBIs. Another problem in analyzing complex breathing patterns is the lack of a neural network model of the respiratory oscillator in the brain stem that could quantitatively describe breathing irregularities in infants.

In this study, we introduced a novel approach to analyze the respiratory pattern in infants. We measured IBIs over a period of 2 h by using a statistical threshold algorithm and found that ***P***(IBI) followed a power law distribution in all infants. ***P***(IBI) can be characterized by a single number, exponent α of the power law, which is the slope of the long tail of the distribution on a log-log plot. Before examining possible mechanisms that can give rise to a power law ***P***(IBI), we first discuss the limitations of our methodology.

Limitations of the Method

Abdominal movement is highly irregular and difficult to describe by using an automated algorithm. The assessment of absolute changes in tidal volume from body surface movements depends on positioning of the motion detectors. However, it should be possible to assess relative changes in abdominal movement without such severe constraints. The use of a threshold algorithm to detect IBIs has advantages and disadvantages. It is certainly optimal to discriminate a tidal breathing excursion from noise (such as that produced by the heartbeat). The absolute abdominal excursion is dependent on the age of the infant, the position of the

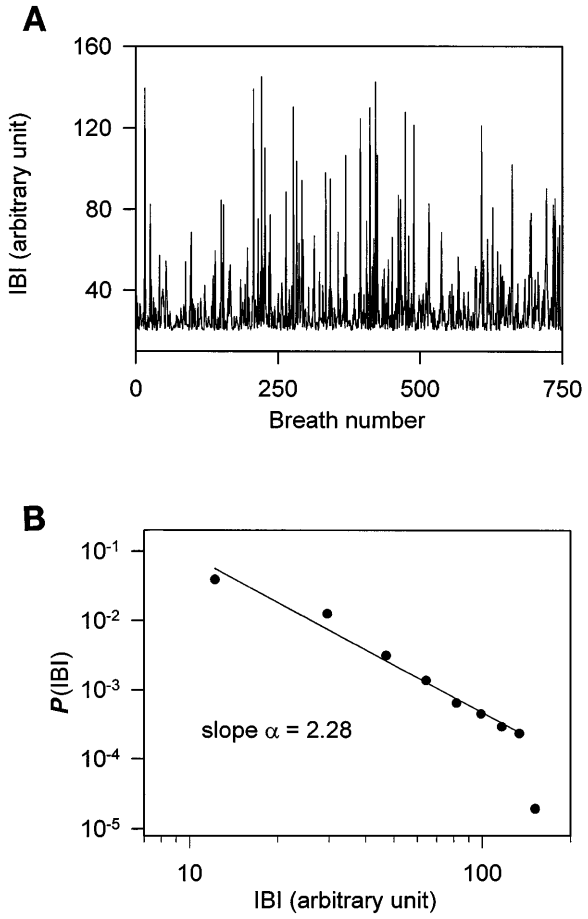

Fig. 6. *A*: computer simulation of IBI time series by using neural network model of respiratory oscillator proposed by Botros and Bruce (4) model (*model A*). Noise introduced in tonic neural input (TNI) of 1st or ramp-inspiratory neuronal group (TNI_1) remains constant over time, SD = 0.07. *B*: ***P***(IBI) of IBI series in *A* follows a power law. Calculations involved 3,000 noise realizations.

infant, and the relative filling of the abdomen. Position and abdominal filling might change during the measurement period. It is also questionable whether a very small tidal excursion should be considered as a breath. To avoid these threshold problems, we chose a statistical approach.

We designed a moving window algorithm, in which the threshold to detect a significant breath is based on the SD of the abdominal tidal excursions within the window. To test the optimal length and stability of the threshold, we simulated the target parameter α as a function of the threshold (Fig. 8*A*) and the time window length (Fig. 8*B*). We found that α was high and ***P***(IBI) was close to a normal distribution if we chose the threshold to be 0 SD above the mean. In this case the IBI pattern was mainly influenced by noise. If the threshold was increased up to 1 SD above the mean of the single window, α decreased rapidly to a value of 3 and remained relatively stable up to a threshold of 1.5 SD, where the power law broke down and only occasional breaths were detected. We chose 1 SD as a threshold that is between these two extremes. The optimal time-window length was determined in a similar way. At time windows over 1 min, α remained stable. A window length of 120 s was optimal because α was stable and the algorithm was still sufficiently flexible to account for slow (>120-s) changes in the absolute value of the abdominal excursion caused by change in posture of the infant or by change in abdominal volume. The use of abdominal movements to assess IBIs seemed justified because the contribution of rib cage movement to tidal volume only seems to change very little in the first 2 yr of life and probably not significantly over the first 5 mo (14). The disadvantage of the algorithm is that it is unable to distinguish between complete apnea and hypopnea with minimal tidal excursion of <1 SD. This makes the algorithm more useful in characterizing the degree of breathing irregularities rather than in detecting an apnea.

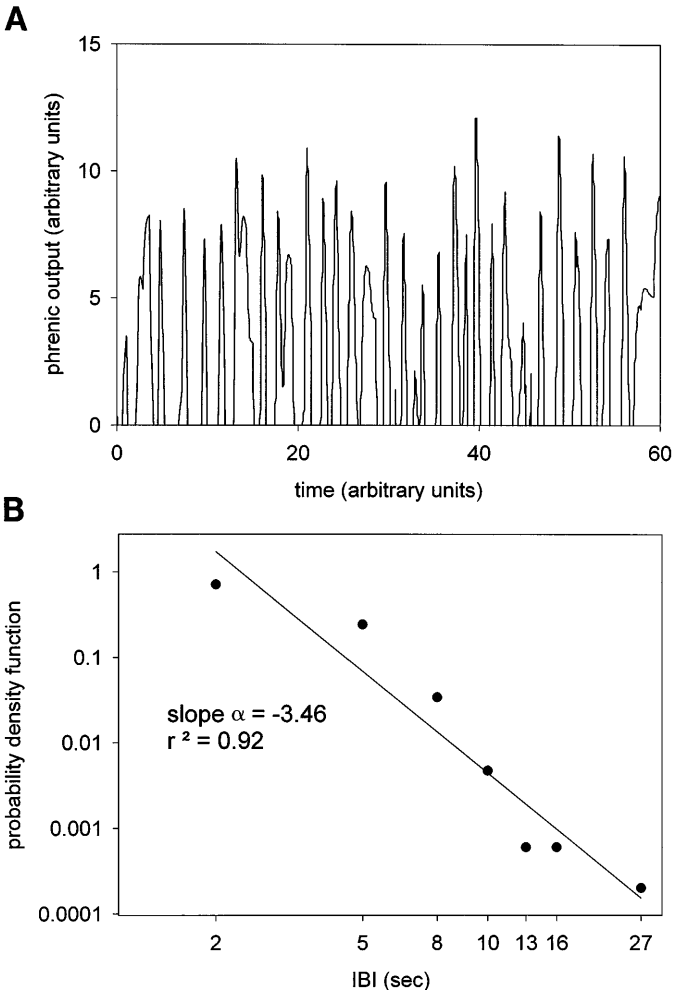

Fig. 7. *A*: computer simulation of phrenic output time series by using neural network model of respiratory oscillator proposed by Botros and Bruce (4) (*model B*). Noise introduced in TNI_1 changes, on average, 4 times within respiratory cycle. *B*: ***P***(IBI) of time series in *A* were analyzed by using threshold algorithm proposed in METHODS. Similar to *model A*, ***P***(IBI) follows a power law. Calculations involved 5,000 noise realizations.

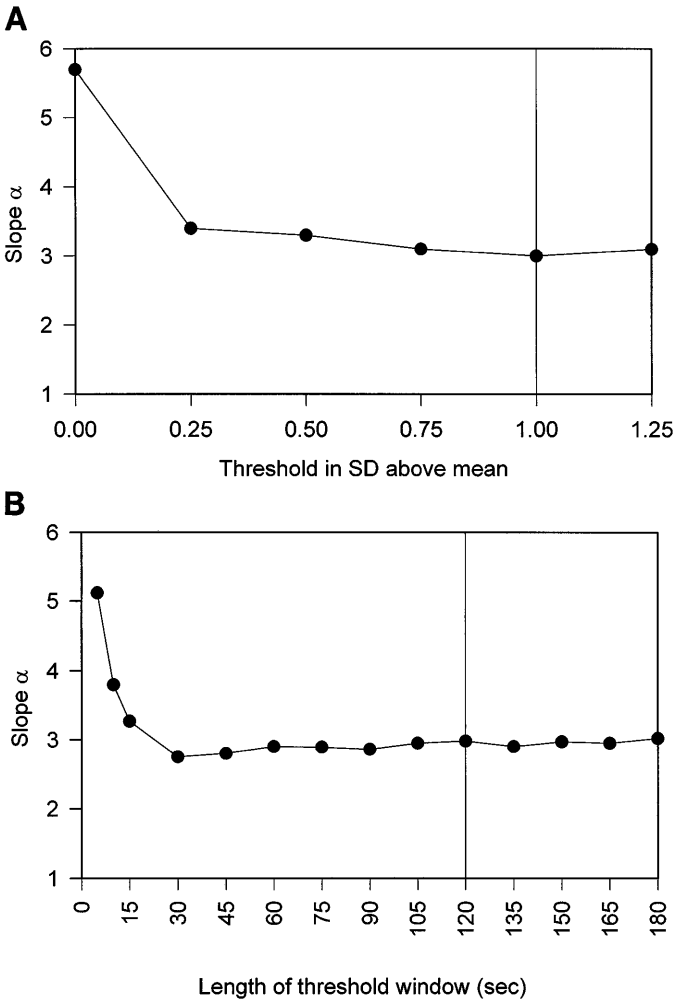

Fig. 8. Robustness of threshold algorithm. Example of exponent α of power law probability density distribution is shown as a function of threshold above mean (*A*) and as a function of length of threshold window (*B*) in a healthy infant. Vertical lines (1 SD, 120 s), optimized specifications.

Central and Obstructive Hypopneas

By measuring the abdominal movements, obstructive hypopnea could be missed. However, most hypopneas involving obstructive components are of mixed type (central and obstructive) (7, 18), which can be detected by this method. If the detection of obstructive hypopneas were the focus of a future study, the same algorithm could potentially be used to analyze nasal flow in a similar way, although abdominal movements are technically easier to assess and therefore more suitable for measurements under natural conditions at home.

Sleep Stages

During a measurement period of 2 h, infants certainly undergo several sleep cycles involving different sleep stages (9). Breathing pattern in infants is dependent on sleep stage (9). The synchrony of chest and abdominal tidal excursions depends on the sleep stage (10). Although our threshold algorithm accounts for slow (>120-s) changes in the relative contribution of chest wall and abdominal movements, a small error might be introduced into the IBI assessment if the abdominal movements are measured during asynchronous paradoxical movements. This error, however, is expected to be minimal if the threshold to detect a breath is chosen at 1 SD above the mean and not close to the mean. To investigate the effect of sleep stage on ***P***(IBI), shorter sampling periods during a single sleep state should be analyzed. This, however, could compromise the reliability of the estimated exponents. We needed to include at least 1,000 IBI values in the calculations of ***P***(IBI). Therefore, the value of α has to be considered as an averaged mean of breathing pattern over several sleep stages. The question arises whether the change in α during maturation is mainly determined by changes in sleep-stage pattern with age. Unfortunately, this question cannot presently be answered. During rapid-eye-movement (REM) sleep, breathing pattern is more irregular. Although the proportion of REM sleep decreases slightly with age in healthy infants (31.6 $\pm$ 6.3% at 3 wk, 24.7 $\pm$ 4.3% at 6 wk, and 28.0 $\pm$ 5.4% at 3 mo of age), the relative amount of quiet sleep changes from 31 $\pm$ 4.6% at 3 wk to 22.5 $\pm$ 8.6% at 3 mo of age (6). A decreased amount of REM sleep with age would theoretically result in more regular breathing, which is consistent with our data; however, this does not explain the fact the IBI irregularities are power law distributed.

Power Law Distribution of IBIs

Power law behavior was found in the breathing patterns in preterm infants as well as term infants. Although α was highly reproducible within the same individual in healthy infants during a single night, the interindividual variability was large in both the heterogeneous group of preterm infants as well as in the healthy term infants. Despite the high interindividual variability, there was a clear tendency for α to increase with PNA in the cross-sectional data set. More importantly, α increased statistically significantly in the longitudinal data sets. This indicates that, although maturation preserved the power law form, α was sensitive to age as an expression of maturation. For small values of α (<3), the tail of ***P***(IBI) extends to large IBIs, and hence the probability that an infant will have a hypopnea much longer than the mean can be orders of magnitude higher than if ***P***(IBI) followed a normal distribution (5). With increasing α, the tail of ***P***(IBI) decreases steeply, and ***P***(IBI) will gradually become closer to a normal distribution. We note that for power law distributions, there is a significant change in the nature of the distribution as α reaches 3. For $\alpha < 3$, the distribution has an infinite second moment (5), and hence it is unbounded and dominated by its power law tail. For $\alpha > 3$, the distribution has a finite second moment (5). Therefore, the distribution has the same general statistical properties as a normal distribution. As a consequence, the occurrence of large IBIs is significantly reduced.

We found that α was sensitive to age in both term and preterm infants. The question is whether prematurity itself influences the power law distribution of IBIs. In a group of preterm infants who had their measurements recorded before PCA of 40 wk, α was significantly lower than in the group of healthy term infants of similar PNA (Table 1). This significance was relatively weak, possibly because the variability of α within the group of preterm infants, representative of daily clinical practice, was rather large.

Various authors have speculated about the origins of power law-distributed time series in biological systems (19, 25, 26). In particular, Szeto et al. (25) measured the distribution of IBIs in fetal lambs. They found that exponent α in ***P***(IBI) ranged from 1.67 to 2.53. This range is close to our α values in preterm infants with low PCA. In contrast to our results, Szeto et al. (25) did not find a clear correlation between α and maturation. The conclusion from their study was that fetal breathing dynamics show fractal characteristics. However, mechanisms that can generate power law ***P***(IBI) and fractal behavior of the IBI time series still remain unclear.

Apparent irregularities in a time series (e.g., in Fig. 2) can be the result of either chaotic behavior or noise in the system. Our data do not support the possibility of chaotic behavior because, except for three subjects with low PCA, the Lyapunov exponents (23) calculated from the IBI time series were negative. We thus hypothesized that introducing appropriate type and amount of noise in a model of the respiratory oscillator in the brain stem may produce variations in IBI and in tidal excursion with statistical properties similar to those obtained from the breathing pattern in infants. There is evidence from animal models that a three-phasic model of the respiratory oscillator is similarly appropriate for describing the breathing cycle in newborns and in adults (17). There is also evidence of noise in the respiratory rhythm generator. The firing of individual neurons has been found to be a probabilistic process with intrinsic noise (1). Recently, Hoop et al. (16)

demonstrated the presence of noise in respiratory-related neural activity in the brain stem of neonatal rats. Thus, to reproduce the observed irregularities, we introduced noise in the neural oscillator model proposed by Botros and Bruce (4).

Our models demonstrate indeed that noise in a neural network oscillator can lead to a power law distribution of IBIs in the breathing pattern and irregularities in tidal volume (see Figs. 6 and 7). We are now in the position to explore what mechanisms in the network oscillator can lead to changes in exponent α similar to those occurring with maturation. One possibility is that the level of noise in the neural network decreases with age in infants. Tonic inputs into the neural network are likely to be related to the vagal feedback from peripheral receptors. It is known that myelination in the vagus nerve in the newborn is a heterogeneous process and increases with age (24). Myelination determines the speed of propagation of action potentials, and hence noise at the effector locus (tonic inputs into the neural network) could occur due to the heterogeneity of transmission times in a nerve consisting of a bundle of parallel neurons. Nevertheless, to our knowledge, there is no direct evidence of decreasing noise during maturation in human infantile neural networks.

Another possibility is that the amplitude of the tonic input into the neural respiratory network changes with maturation. Indeed, Sachis et al. (24) postulated that with increasing myelination the input from the vagus nerve into the respiratory oscillator may become stronger in older infants in comparison with immature young infants. Indirect evidence in human infantile brain stem function may be derived from the auditory system, which is in a neighborhood close to the respiratory oscillator and shows increasing amplitudes of acoustic-evoked potentials with age (13). Further evidence might be derived from intracellular recordings in the respiratory center of the brain stem of newborn piglets (17). We wondered, therefore, whether changes in the amplitudes of tonic inputs into the neural respiratory network could explain changes in α.

In a noise-free case, IBI becomes a function of the amplitude of TNI_1. Examining the input-output (TNI_1-IBI) relationship of the respiratory oscillator model, we found that, as TNI_1 decreases, the IBI becomes excessively longer, reaching a critical region where IBI diverges. If we add a uniformly distributed noise to TNI_1 so that it explores this critical region of the oscillator where IBI diverges, i.e., it is subject to a power law transformation with exponent μ, then the resulting fluctuations in IBI will have a power law distribution with exponent $\alpha = 1 + 1/\mu$ (2). Although the TNI_1-IBI curve in Fig. 9 is not exactly a power law, if the SD of the noise is small, then, in the vicinity of the mean of TNI_1, a power law fit of the form $IBI = A*(TNI_1)^{\mu}$ is a reasonable approximation (Fig. 9, *inset*). Thus, for small SD, the uniform noise in TNI_1 is transformed into a power law-distributed noise. However, exponent α obtained from the simulations may be slightly different from the theoretical $\alpha = 1 + 1/\mu$ relationship, being determined by the average of the local slopes on the TNI_1-IBI curve sampled by TNI_1. Our model is also capable of accounting for maturation. Increasing the mean of TNI_1 results in a decreasing μ (Fig. 9), which in turn increases α. Accordingly, we conclude that during maturation TNI_1 may become larger in accordance with Sachis et al. (24), resulting in a shift of the mean of TNI_1 away from the region where IBI diverges. Indeed, if we increase the mean TNI_1 in *model A*, we find again a power law-distributed IBI time series with $\alpha = 3.57$, which is in excellent agreement with $\boldsymbol{P}$(IBI) in Fig. 3 at PCA = 61 wk.

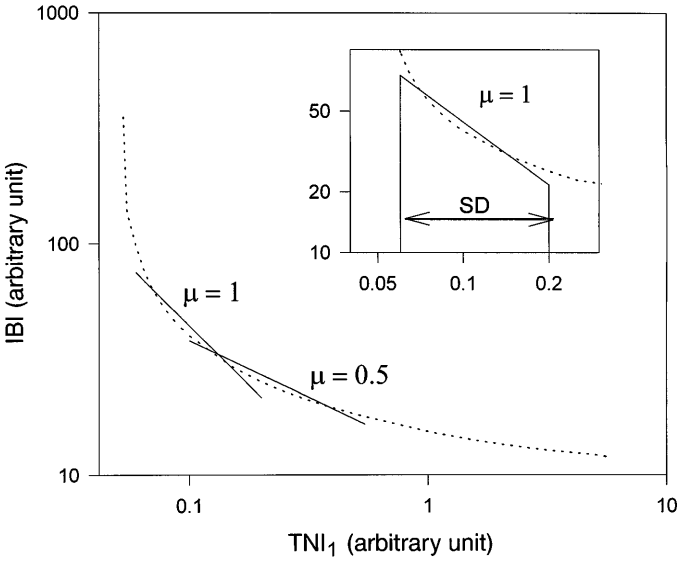

Fig. 9. IBI as a function of TNI_1 diverges as TNI_1 is decreased. In vicinity of $TNI_1 = 0.12$ a power law reasonably fits that part of singularity curve that is sampled by noisy TNI_1 with SD = 0.1 (*inset*). Slope of this fit, μ, is 1, which, according to theoretical $\alpha = 1 + 1/\mu$ relationship (see Ref. 2), predicts $\alpha = 2$. Also, note that moving mean of TNI_1 away from singularity to $TIN_1 = 0.3$ results in $\mu = 0.5$ and $\alpha = 3$.

Before physiological conclusions can be drawn, we note the following. The correspondence between the various neural functions and the parameters of the model is relatively well understood (4, 20–22), and the original model accounts for much of the neurophysiology of respiratory control in newborns (8, 17). However, the influence of the various chemoreceptor and stretch-receptor inputs on TNI is heterogeneous and cannot be separated easily. Although the above mechanism of noise operating on TNI_1, which is a function of maturation, can quantitatively explain the changes in α with age as an expression of maturation, there could, of course, be a number of other factors influencing $\boldsymbol{P}$(IBI) and α. For example, we only examined the effect of tonic input to the ramp-inspiratory neuronal group. Other tonic inputs simultaneously varying within the respiratory cycle would certainly influence IBI. Additionally, we used white noise, whereas it has been observed that noise in respiratory neurons is correlated (16). The amount of time correlation in the noise may also affect the IBIs because this correlation would determine how much time, on average, the oscillator would spend in the neighborhood of the critical region where IBI diverges. Because of the complicated interactions of all

these effects, in this study our goal was to demonstrate how irregularities in IBI can lead to a power law $\boldsymbol{P}(\mathrm{IBI})$ and how exponent α can be related to the neurophysiology of the oscillator.

In conclusion, we characterized the complex pattern of infant breathing with a single number, α, which facilitates the analysis of easily accessible data in infants. Because α is sensitive to age as an expression of maturation and because α can easily be measured even under home-based-monitoring conditions, it has the potential to be used as a simple index for evaluating the likelihood of long hypopneas in various groups of infants, i.e., infants with inherited or acquired neurodevelopmental problems, such as preterm infants, infants suffering from birth asphyxia, or those who are at risk for sudden infant death syndrome for other reasons. We also provided a computational model that can explain how the respiratory neural oscillator network produces irregularities in breathing frequency and tidal amplitude with power law properties. Future studies will be necessary to find links between neurophysiological mechanisms of respiratory control and clinically accessible measurements of the complex breathing pattern.

We thank J. J. Collins for helpful comments and J. Westaway, K. Sleath, A. Jackson, and D. Milner for help during data acquisition.

This work was supported by the Swiss National Science Foundation (U. Frey), by the National Science Foundation (B. Suki), and by the British Society for the Protection of Infants' Life.

Address for correspondence and reprint requests: U. Frey, Paediatric Respiratory Medicine, Dept. of Paediatrics, Univ. Hospital of Berne, Inselspital, 3010 Berne, Switzerland (E-mail: urs.frey@insel.ch).

Received 5 December 1996; accepted in final form 20 April 1998.

REFERENCES

1. **Amit, D. J.** *Modeling Brain Function: The World of Attractor Neural Networks*. Cambridge, UK: Cambridge Univ. Press, 1989.
2. **Barabási, A.-L., and H. E. Stanley.** *Fractal Concepts in Surface Growth*. Cambridge, UK: Cambridge Univ. Press, 1995.
3. **Bergman, A. B., C. G. Ray, M. A. Pomeray, P. W. Wahl, and J. B. Beckwith.** Studies of the sudden death syndrome in King County, Washington. III. Epidemiology. *Pediatrics* 49: 860–870, 1972.
4. **Botros, S. M., and E. N. Bruce.** Neural network implementation of a three phase model of respiratory rhythm generation. *Biol. Cybern*. 63: 143–153, 1990.
5. **Bouchaud, J. P., and A. Georges.** Anomalous diffusion in disordered media—statistical mechanism, models and physical applications. *Physiol. Res.* 195: 127–293, 1990.
6. **Coons, S., and C. Guilleminault.** Development of sleep wake patterns and non-rapid-eye-movement sleep stages during the first 6 month of life in normal infants. *Pediatrics* 69: 793–798, 1982.
7. **Dransfield, D. A., A. R. Spitzer, and W. W. Fox.** Episodic airway obstruction in premature infants. *Am. J. Dis. Child*. 137: 441–443, 1983.
8. **Farber, J. P.** Medullary inspiratory activity during opossum development. *Am. J. Physiol*. 254 (*Regulatory Integrative Comp. Physiol*. 23): R578–R584, 1988.
9. **Finer, N. N., I. F. Abrams, and H. W. Tauesch.** Ventillation and sleep states in newborn infants. *J. Paediatr. Child Health* 89: 249–254, 1976.
10. **Gaultier, C., J. P. Praud, E. Canet, M. F. Delaperche, and A. M. d'Allest.** Paradoxical inward rip cage motion during rapid eye movement sleep in infants and young children. *J. Dev. Physiol. (Eynsham)* 9: 391–397, 1987.
11. **Gerhardt, T., and E. Bancalari.** Apnea of prematurity: lung function and regulation of breathing. *Pediatrics* 74: 58–62, 1984.
12. **Girard, F., A. Lacaisse, and P. Dejours.** Le stimulus O_2 ventillatoire à la période neonatale chez l'homme. *J. Physiol. Paris* 52: 108–109, 1960.
13. **Henderson-Smart, D. J., A. G. Pettygrew, and D. J. Campell.** Clinical apnea and brainstem neural function in pretem infants. *N. Engl. J. Med*. 308: 353–357, 1983.
14. **Hershenson, M. B., A. A. Colin, M. E. B. Wohl, and A. R. Stark.** Changes in the contribution of the rib cage to tidal breathing during infancy. *Am. Rev. Respir. Dis*. 141: 922–925, 1990.
15. **Hodgman, J. E., F. Gonzales, T. Hoppenbroewers, and L. A. Cabal.** Apnea, transient episodes of bradycardia and periodic breathing in preterm infants. *Am. J. Dis. Child*. 144: 54–57, 1990.
16. **Hoop, B., M. D. Burton, H. Kazemi, and L. S. Liebovitch.** Correlation in stimulated respiratory neural noise. *Chaos* 5: 609–613, 1995.
17. **Lawson, E. E., D. W Richter, and A. M. Bischoff.** Intracellular recordings of respiratory neurons in the lateral medulla of piglets. *J. Appl. Physiol*. 66: 983–988, 1989.
18. **Mathew, O. P., J. L. Roberts, and B. T. Thach.** Pharyngeal airway obstruction in preterm infants during mixed and obstructive apnea. *J. Pediatr*. 100: 964–968, 1985.
19. **Montroll, E. W., and M. F. Schlesinger.** On 1/f noise and distributions with long tails. *Proc. Natl. Acad. Sci. USA* 79: 3380–3383, 1982.
20. **Ogilvie, M. D., A. Gottschalk, K. Andersm, D. W. Richter, and A. I. Pack.** A network model of respiratory rythmogenesis. *Am. J. Physiol*. 263 (*Regulatory Integrative Comp. Physiol*. 32): R962–R975, 1992.
21. **Paydarfar, D., and D. M. Buerkel.** Dysarythmias of the respiratory oscillator. *Chaos* 5: 18–29, 1995.
22. **Richter, D. W., and D. Ballantyne.** A three phase theory about the basic respiratory pattern generator. In: *Central Neurone Environment*, edited by M. E. Schlafke, H. P. Koepchen, and W. R. See. Berlin: Springer-Verlag, 1983, p. 165–174.
23. **Rosenstein, M. T., J. J. Collins., and C. J. De Luca.** A practical method for calculating largest Lyapunov exponents for small datasets. *Physica D*. 65: 117–134, 1993.
24. **Sachis, P. N., D. L. Armstrong, L. E. Becker, and A. C. Bryan.** The vagus nerve and sudden infant death syndrome: a morphometric study. *J. Neuropathol. Exp. Neurol*. 41: 466–472, 1982.
25. **Szeto, H. H., P. J. Cheng, J. A. Decena, Y. I. Cheng, D.-L. Wu, and G. Dwyer.** Fractal properties in fetal breathing dynamics. *Am. J. Physiol*. 263 (*Regulatory Integrative Comp. Physiol*. 32): R141–R147, 1992.
26. **Suki, B., A.-L. Barabási, Z. Hantos, F. Peták, and H. E. Stanley.** Threshold phenomena, avalanches and power law distributions in airway openings. *Nature* 368: 615–618, 1994.